

Local-density approximation for confined bosons in an optical lattice

Sara Bergkvist,* Patrik Henelius, and Anders Rosengren
*Condensed Matter Theory, Physics Department, KTH,
 AlbaNova University Center, SE-106 91 Stockholm, Sweden*
 (Dated: November 1, 2018)

We investigate local and global properties of the one-dimensional Bose-Hubbard model with an external confining potential, describing an atomic condensate in an optical lattice. Using quantum Monte Carlo techniques we demonstrate that a local-density approximation, which relates the unconfined and the confined model, yields quantitatively correct results in most of the interesting parameter range. We also examine claims of universal behavior in the confined system, and demonstrate the origin of a previously calculated fine structure in the experimentally accessible momentum distribution.

PACS numbers:

I. INTRODUCTION

When a system of cold atoms confined in an external trap is exposed to a standing-wave laser field the electric field couples to the dipole moments of the atoms and a so-called optical lattice is created. A system of trapped bosonic atoms in such a lattice is expected to be well described by a Bose-Hubbard model.¹ The phase diagram of the homogeneous Bose-Hubbard model was obtained by Fisher *et al.*,² and confirmed by quantum Monte Carlo investigations.³ The model exhibits two possible phases for large on-site interaction between the atoms. At commensurate filling there is a Mott insulating phase and at non-commensurate fillings there is a superfluid phase. The optical lattices constitute a new realization of the Hubbard model, and offer an unprecedented control of most model parameters such as lattice size, dimension, chemical potential, and the intersite coupling. Using this high degree of control Greiner *et al.* have recently studied the release of atoms from an optical lattice.⁴ In an absorption measurement they studied the momentum distribution and detected a gradual decrease of the center peak in the absorption spectra with an increase in the on-site interaction between atoms, indicating a growing Mott insulating phase in the center of the trap. The need to interpret and understand this, and related, recent experiments performed in optical lattices have renewed interest in understanding various extensions of the well-studied bosonic Hubbard model.

In the case of optical lattices the picture is complicated by the trapping potential. The trapping potential is an external potential applied to keep the atoms in the lattice. Due to the spatial variation of the confining potential, different phases can be realized in different parts of the trap, leading to a spatial phase separation. This has been demonstrated using quantum Monte Carlo techniques for bosons⁵ and fermions.^{6,7} These studies focused on the differences between the phase diagram of the confined and unconfined model and calculated state-diagrams for the confined model. A density matrix renormalization group study⁸ shows that the decay of correlation functions in the confined case can be

easily rescaled to obtain the form expected for the homogeneous model. These results were also shown to agree very well with a hydrodynamical treatment of the 1D Bose gas combined with a local density approach. Results for large systems have also been obtained by combining the Gutzwiller mean-field ansatz with a numerical renormalization group procedure.⁹ Recent large-scale Monte Carlo studies^{10,11} extend previous work to higher dimensions and address questions of critical behavior and local order parameters.

In this work we focus on the similarities of the phase diagram for the unconfined and the confined state diagram. We map the site-dependent confining potential for the trapped system to the chemical potential for the homogeneous system and in this manner determine the properties of the confined system in a local-density approximation. It is reasonable to believe that a good agreement between the confined and the unconfined system is obtained for local observables in weakly interacting systems, where the correlation length is short. Here we demonstrate that the approximation can be used with good accuracy in most of the range of interactions where the Mott insulating phases appear. Furthermore, the approximation can be used also for the nonlocal momentum distribution, which is calculated from the particle-particle correlation function. This local-density approximation has been used to compare a number of observables previously,^{5,6,7,9,10,11} but here we present a more exhaustive comparison of several observables. One practical aspect of the local-density approximation is that it allows a very quick estimate of the distribution of different phases in a specific trap setting from knowledge of only the phase diagram of the homogeneous model.

The outline of the paper is as follows. In Sec. II we discuss the phase diagram for the Bose-Hubbard model and explain the mapping between the confined and the unconfined model. In Sec. III we briefly discuss the Monte Carlo method and present results testing the validity of the local-density approximation. We conclude with a summary and conclusions.

II. BOSONS IN AN OPTICAL LATTICE

Starting from a general Hamilton operator for bosonic atoms in an external trapping potential and optical lattice, Jaksch *et al.*¹ expand the bosonic field operators in the Wannier basis and arrive at the Bose-Hubbard model. In order to review the properties of this fundamental model we start by disregarding the effects of the confining potential and consider the homogeneous one-dimensional Bose-Hubbard model,

$$H_{BH} = \sum_i -t(c_i^\dagger c_{i+1} + \text{H.c.}) + \frac{V}{2}n_i(n_i - 1) - \mu n_i, \quad (1)$$

where t is the hopping matrix element between adjacent sites, V is the on-site repulsion, μ is the chemical potential, and n_i is the number of bosons at site i . At zero temperature there are two possible phases for the model. For small on-site repulsion the kinetic energy is minimized by a phase coherent superfluid phase, characterized by a nonzero superfluid density, algebraically decaying correlation functions and a linear, gapless excitation spectrum. As the on-site repulsion is increased it becomes harder for the bosons to move, due to the increasing potential energy cost. At a critical value of the on-site repulsion the model enters the Mott insulating phase where each lattice site is filled with the same number of bosons. The suppression of the fluctuations in particle number makes the Mott insulating phase incompressible with a vanishing compressibility, $\kappa = \beta(\langle n^2 \rangle - \langle n \rangle^2) = 0$. The insulating phase is gapped and correlation functions decay exponentially. The zero-temperature phase diagram for the Bose-Hubbard model, as a function of density and the hopping parameter t/V , is schematically shown in the right part of Fig. 1. For small values of t/V there is a series of Mott lobes as the density is increased. In each Mott lobe the system is in the insulating phase and the density is constant. At large values of t/V the model is in the superfluid phase.²

As shown by Jaksch *et al.*¹ the Bose-Hubbard model is an effective model for a Bose-Einstein condensate of atoms when subjected to an optical lattice potential. The potential energy is given by $V = 4\pi a_s \hbar \int d^3x |w(x)|^4/m$, where a_s is the s -wave scattering length, $w(x)$ is a localized Wannier function and m is the atomic mass. As the lattice potential is turned on the condensate remains in a superfluid state for small values of the potential. However, as the potential is increased there is a transition to an insulating phase where the phase coherence of the condensate is destroyed, as demonstrated by Greiner *et al.*⁴ Other properties of the Mott insulating phase, such as the robustness to external perturbations due to the excitation gap have also been verified experimentally.⁴ The relevance of the Bose-Hubbard model to Bose-Einstein condensates have therefore been demonstrated both experimentally and theoretically, and in this work we examine the model further using quantum Monte Carlo simulations. Some of the quantities we examine, such as

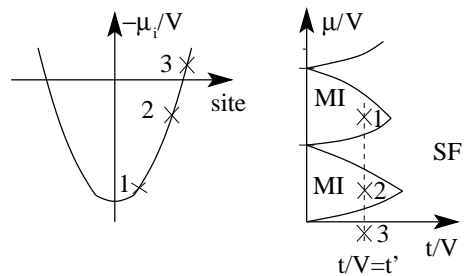


FIG. 1: Demonstration of the local-density approximation where a system with a confining potential is mapped to a slice in the phase diagram for the Bose-Hubbard model. The figure to the left represents the site dependent potential μ_i/V as a function of lattice site for a confined system with hopping parameter $t/V = t'$. The figure to the right shows a schematic phase diagram for the unconfined Bose-Hubbard model, where the insulating Mott lobes (MI) and superfluid phase (SF) are indicated. The dashed line in the phase diagram represents the different values of the effective chemical potential obtained in the confined system. The three x's mark how three specific sites in the confined system are mapped to the phase diagram on the right.

the density profile of bosons in the trap, or the momentum distribution of the bosons, can be directly measured experimentally. Other quantities, such as local-density fluctuations may be harder to observe experimentally, but are of interest since they tell us how the superfluid-insulator transition occurs in a confined system.

In experimental realizations of the optical lattice a confining potential is necessary to prevent the bosons from escaping. The confinement typically spans a couple of hundred lattice sites and its strength is adjusted to be large enough so that there are no atoms at its edges. The confining potential is also used to control the dimensionality of the system. By using a very narrow confinement in some directions the dimensionality of the system is changed. In this work we consider a setup with a narrow confinement in two dimensions and a broad confining potential in one dimension, leaving a one-dimensional system. The broad confining potential adds a site dependent potential term to the Hamiltonian

$$\begin{aligned} H &= H_{BH} + U_c \sum_i \left| i - \frac{N}{2} \right|^\alpha n_i \\ &= \sum_i -t(c_i^\dagger c_{i+1} + \text{H.c.}) + \frac{V}{2}n_i(n_i - 1) - \mu_i n_i, \end{aligned} \quad (2)$$

where α is a parameter that controls the power of the confining potential. In the second line of the equation the confining potential and the chemical potential μ are combined into a site dependent chemical potential, μ_i . Different sites in the lattice therefore have different effective chemical potentials. In the limit of vanishing t the local properties of the system are determined by the value of the local chemical potential. For finite values of t/V

we assume that the local properties of the confined system may be obtained from a homogeneous system with the same value of t/V as in the confined system, and a chemical potential equal to the effective chemical potential at the point considered in the confined lattice. This mapping is illustrated in Fig. 1 where it is shown how the confined system represents a constant t/V slice in the $\mu - t$ diagram of the homogeneous system.

We examine the accuracy of this local-density approximation for a range of hopping parameters where the Mott insulating phases are present. In general we expect poor results for very deep and narrow traps where the potential varies rapidly from site to site and close to phase transitions where the correlation length diverges in the unconfined system. At a true phase transition the correlation length diverges, but due to the limited size of the confined system the correlation length cannot diverge and there cannot be a true phase transition. We merely expect a system with spatially separated regions of different phases, a scenario which is supported by our results. A careful analysis of the lack of critical behavior can also be found in Refs. [10,11].

The trap used in the experiment described by Greiner was of size $65 \times 65 \times 65$ and contained a maximum of 2.5 bosons per site. In this work we consider one-dimensional traps with a linear size of about 300 sites and a density up to two bosons per site. Therefore, we believe that the results we obtain are pertinent to recent experimental setups.

III. RESULTS

In this work we use the stochastic series expansion quantum Monte Carlo method.^{12,13} We perform the calculations at a fairly low temperature of $\beta/V = 256$, and the convergence is controlled with a calculation at a temperature of half this value.

We study the densities in a trap with a linear, square, and a quartic potential, i.e. $\alpha = 1, 2$, and 4 in Eq. (3). The calculation is performed for three different values of the hopping parameter, $t = 0.05, 0.1$, and 0.2 . We mainly show results for the two cases $t = 0.1$ and 0.2 , since $t = 0.05$ and $t = 0.1$ yield quantitatively very similar results. The on-site repulsion V is set to one. The strength of the confining potential U_c , and the chemical potential μ , are adjusted so that the effective chemical potential $\mu_i/V = 1$ in the center of the well, and is large enough to ensure that there are no bosons at the edges of the trap.

In Fig. 2 we display the approximate phase diagram of the homogeneous Bose-Hubbard model, based on Fig. 5 in Ref. [14] and Fig. 9 in Ref. [15]. In the phase diagram we indicate the three slices at fixed value of the hopping t/V that our confined models represent. We note that the slices at $t/V = 0.05$ and $t/V = 0.1$ cut through a significant part of the first Mott lobe, while $t/V = 0.2$ is chosen to cut through the tip of the same lobe.

The local-density as a function of lattice site is shown

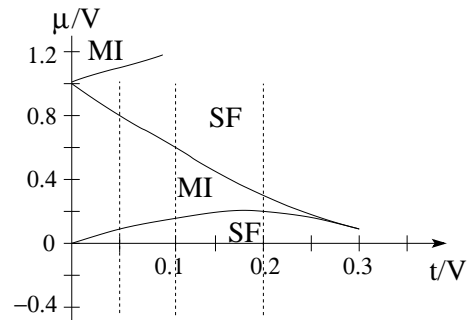


FIG. 2: A detailed phase diagram showing the first Mott lobe (MI) and the surrounding superfluid phase (SF). The chemical potential μ/V is plotted as a function of the hopping parameter t/V . The three slices of the $\mu - t$ diagram that our confined systems represent are indicated with the dotted lines. The dotted lines start at a μ low enough to ensure that there are no atoms at the edges of the trap, and they all end at $\mu/V = 1$.

in Fig. 3. We note that for $t = 0.1$ there is a range of lattice sites for which the local-density takes the value of one boson per site for all three confining potentials. Since the density fluctuations are strongly suppressed in these regions they appear incompressible and are therefore called Mott plateaus, indicating that the system is in a Mott insulating state. For $t = 0.2$ there is not yet a well defined plateau, but all three density curves corresponding to the three different confining potentials display a slight kink at unit density.

If the densities at different lattice sites are presented as a function of the effective on-site chemical potential, this density can be directly compared with the density in a homogeneous system with the same value of the chemical potential. The results are shown in Fig. 4, and we see a good quantitative agreement between the densities for the confined and the unconfined systems for most of the parameter regime. Due to the diverging correlation function there is some discrepancy close to the place where there is a phase separation between the Mott insulating regions and the superfluid phases, which is shown in the insets. The sharp edge for the homogeneous system is simply smoothed out, indicating the absence of a true phase transition as the plateau is approached in the confined system. In the lower part of the figure, which presents results for $t/V = 0.2$, one can see that there is a small plateau in the homogeneous case, which is smeared out in the confined systems. This indicates that there is no true Mott insulating region in the confined system even though the unconfined system has a Mott insulating phase. We also can detect a small difference close to the edge of the trap, where the local-density decreases quite rapidly from site to site.

The Mott insulating phase is incompressible, and the global compressibility vanishes in the Mott insulating phase for the unconfined system. For the confined system the global compressibility never vanishes⁵ since there are

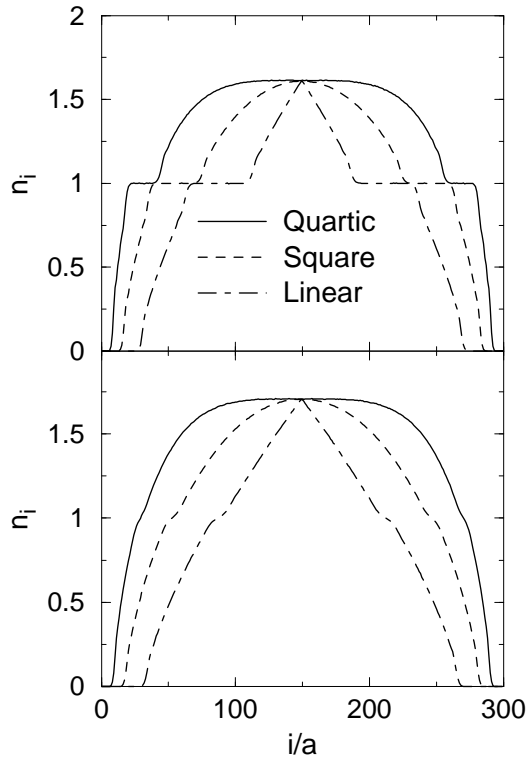


FIG. 3: The local-density n_i as function of lattice sites for three different confining potentials. The upper figure is calculated for $t/V = 0.1$ and the lower for $t/V = 0.2$. The lattice constant is denoted by a .

always superfluid regions present. Here we examine the behavior of a local compressibility, defined as the fluctuations in the local-density

$$\Delta_i^2 = \langle n_i^2 \rangle - \langle n_i \rangle^2. \quad (3)$$

The results are presented in Fig. 5 where we once again compare the result for the confined system with values obtained for the unconfined case. Again we notice a good general agreement, but discrepancies close to the edge of the plateaus and particularly at the edge of the trap. The quartic potential rises faster than the other potentials at the boundary of the trap, and it is also in the data for the quartic potential that we see the largest deviations from the homogeneous case. For $t = 0.2$ the inset shows the deviations in the region where the homogeneous system forms a Mott plateau. This is another indication that the confined system does not manage to form a well developed insulator here, as mentioned above in the argumentation about the density profile. This has previously been noted for the case of fermionic systems.⁷

Next we focus on the properties of the system as a plateau is approached. As a Mott plateau is entered by scanning the chemical potential for the homogeneous system there is a second-order phase transition from the superfluid to the Mott insulating phase. In the confined

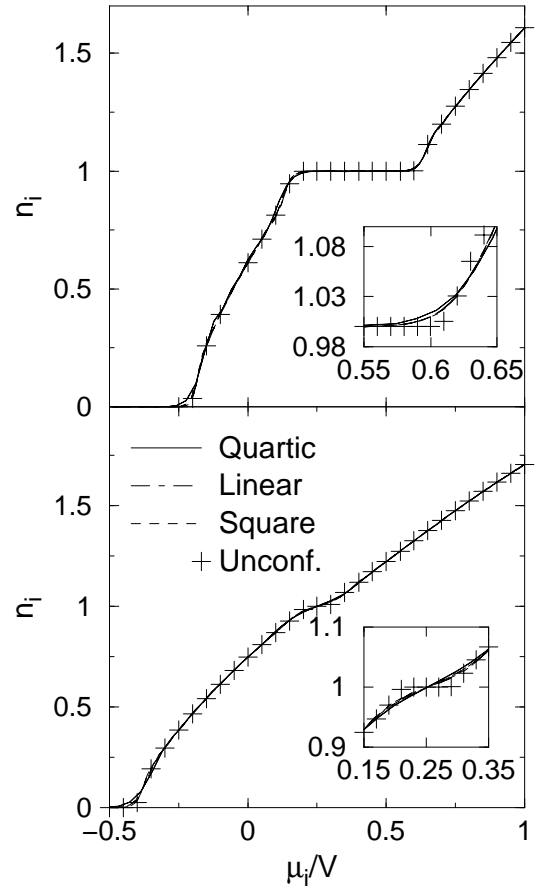


FIG. 4: A comparison of the densities for the confined and unconfined case. The local-density n_i is plotted as a function of the effective chemical potential μ_i/V . Note that the results for the quartic, linear, and square potentials essentially coincide with each other, and with the results for the unconfined system. The insets show the region around points where there is a phase transition for the homogeneous system. In the upper figure $t/V = 0.1$ and in the lower figure $t/V = 0.2$.

system, at least in one dimension, there can be no true phase transition since there cannot be a divergent correlation length at the boundary between the two phases, and we simply have a system displaying spatial phase separation. A similar conclusion was also reached for a two-dimensional system.^{10,11} Nevertheless, there have been claims of universal behavior as a Mott plateau is approached.^{5,6} In Ref. [5] it was argued that the variance in the local-density shows universal behavior as the Mott plateau is approached. This behavior was not reproduced in a numerical renormalization group study⁹, and in Fig. 6 we display the variance in the local-density as the Mott lobe is approached for three different values of the hopping parameter. By analyzing the data in Fig. 6 more closely we find that the local-density approximation works very well, in contrast to the fermionic case.⁶ The accuracy of the local-density approximation probably explains the “universal” behavior seen previ-

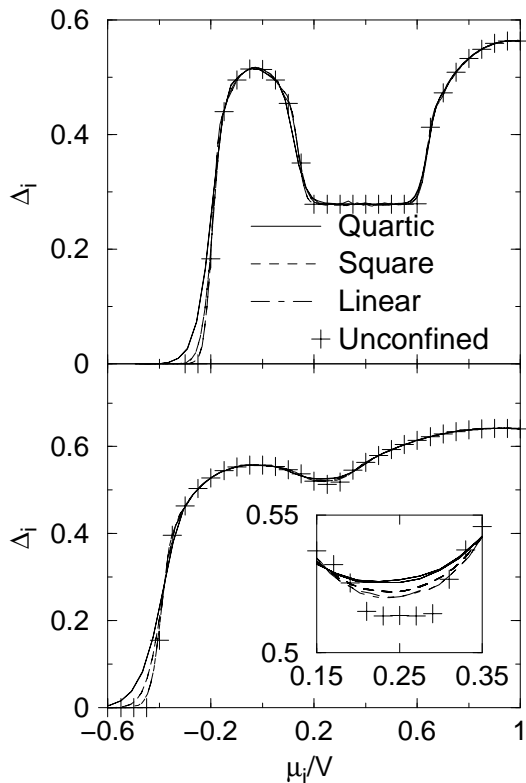


FIG. 5: Variance in the local-density Δ_i as a function of the effective potential μ_i/V for different confining potentials and also for the unconfined system. In the upper figure $t/V = 0.1$ and in the lower figure $t/V = 0.2$.

ously. However, as t is varied the curves readily separate and there is thus no real universality.

Another case of universality as the Mott plateau is approached in a confined system has been reported⁶ for a different definition of a local compressibility,

$$\kappa_i^l = \sum_{|j| \leq l} \langle n_i n_{i+j} \rangle - \langle n_i \rangle \langle n_{i+j} \rangle, \quad (4)$$

which reflects the response at site i to a change in the chemical potential in a region of size l . This compressibility was introduced as a local order parameter, which vanishes in the insulating phase. It was also argued that this compressibility decays with a universal power law as a Mott plateau is approached in a fermionic system. We investigate this quantity for a bosonic system. The value of l is somewhat arbitrary and was previously chosen to be larger than the correlation length in the insulating phase. Here we take the sum over the entire system, to remove the uncertainty associated with the size of l , and hereafter we remove the index l . The compressibility still behaves in essentially the same way as if we limit the sum to some smaller region.

Extending the range of the summation makes the definition of the local compressibility identical to the definition used in Refs. [10,11], and the sum of the local

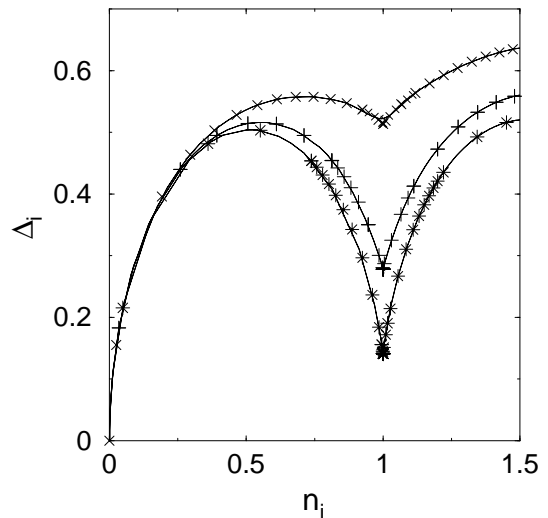


FIG. 6: Variance in the local-density Δ_i as a function of density for the unconfined case [$t/V = 0.05$ (*), $t/V = 0.1$ (+), $t/V = 0.2$ (\times)]. The solid line shows results for the confined system with a square potential.

compressibility at all sites is the global compressibility. This compressibility diverges for the homogeneous system as the phase transition is approached from the superfluid phase, and is zero in the insulating phase, as mentioned above. Finite-size effects prevent the compressibility from diverging in a finite system, and instead the compressibility approaches zero as a smooth function as the insulating state is entered. The way in which the local compressibility approaches zero in a finite but unconfined system is therefore a finite-size effect.

In Fig. 7 we show this decay of the local compressibility as the Mott insulator is approached. It appears that the compressibility decays algebraically as we approach the Mott plateau, which is the behavior described for the fermionic system⁶. The exponent is very similar for the different strengths of the hopping. However, we also note that the compressibility for the homogeneous system follows the same behavior as the confined system, in contrast to the behavior depicted for the fermionic case. It appears that this algebraic decay is not the result of universal behavior as a Mott plateau is approached in the confined system, but rather another property of the homogeneous model that carries over to the confined system. It is reasonable that the confined and the unconfined model display the same type of finite-size effects, and therefore the observed similarity between the confined and the unconfined system is expected. In the bosonic case we find that the exponent that describes the decay has a numerical value of about 1.0, as compared to about 0.7-0.8 in the fermionic case.⁶ The exponent appears slightly smaller for the confined systems, but the statistical fluctuations are larger in this case, which probably explains the small difference. The same exponent is

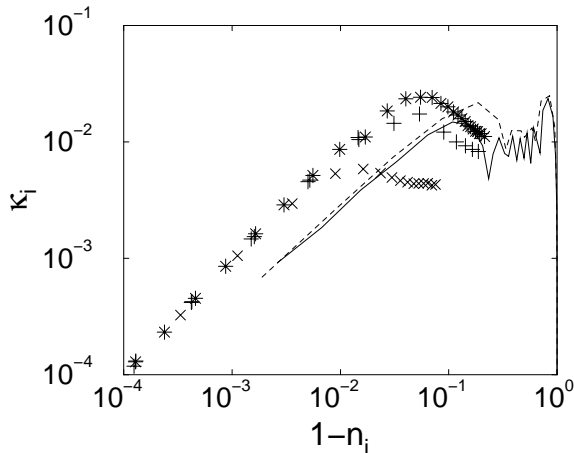


FIG. 7: Local compressibility κ_i for the unconfined case [$t/V = 0.05$ (*), $t/V = 0.1$ (+), $t/V = 0.2$ (x)] and the confined system with a square potential [$t/V = 0.05$ (dashed line), $t/V = 0.1$ (solid line)].

obtained if we analyze the transition to zero density at the edge of the trap, which is expected since this is the same kind of phase transition.

We have done a short calculation for the fermionic system and we found that for both the unconfined and the confined systems the local compressibility decays to zero in an algebraic manner. This is different from the previously reported behavior⁶, described above, where only the confined system displays such a decay. A possible reason for the discrepancy is that we use a grand canonical ensemble, instead of a canonical ensemble, which seems to be more appropriate when observing particle number fluctuations. We found that the exponent for the unconfined model is very close to one and that the confined model may have the same, or a slightly, smaller exponent.

By releasing the atoms in the trap the momentum distribution, n_k , can be obtained experimentally.⁴ This is probably the most accessible observable that can be studied both experimentally and theoretically. The momentum distribution is the Fourier transform of the particle-particle correlation function,

$$n_k = \sum_{i,j} \exp^{ik(r_i - r_j)} \langle c_i^\dagger c_j \rangle. \quad (5)$$

In the homogeneous model the particle-particle correlation function is expected to decay algebraically in the superfluid phase, while it decays exponentially in the insulating phase. By a simple rescaling this has been demonstrated also for the trapped system.⁸

In Fig. 8 we show the particle-particle correlation function from a few selected points in the trapped system. We can clearly see the exponential decay of the correlation function within the insulating phase, and the much slower decay in the superfluid phase. We also note that correlation functions from points in the superfluid regions decay exponentially as they enter the Mott insulating regions. Especially interesting are points close to the phase

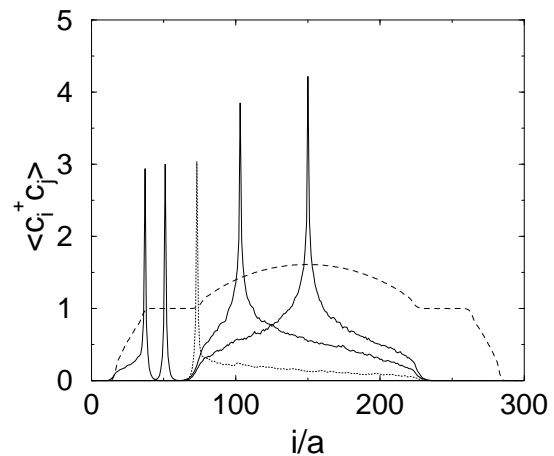


FIG. 8: The particle-particle correlation function $\langle c_i^\dagger c_j \rangle$ for a few selected lattice points i to all other points j in the lattice. The dashed line represents the density profile, shown here to indicate the location of the Mott insulating phases. The dotted line marks the correlation function from a point on the phase separation boundary between the super fluid and Mott insulating regions.

separation boundary. The dotted line represents the correlation function from such a point, which displays exponential decay on one side and a long-range algebraic decay on the other side.

To obtain the momentum distribution we first average the particle-particle correlation function over the whole system. In Fig. 9 the sum of all the particle-particle correlation functions is presented. This function is compared with the function obtained if the correlation functions for different μ -values for the homogeneous system are added. The chemical potentials are chosen with equal spacing in the whole range covered by the effective potential in the well. The sum can immediately be compared with the total correlation function for the system with a linear confining potential. However, for the other potentials the correlation functions have to be reweighted since we use equally spaced values of the chemical potential in the homogeneous system. To reweight the correlation function we multiply the distribution with the derivative of the confining potential with respect to i , the lattice position. We notice that the agreement is very good for small distances, while the correlation function for the homogeneous system has a longer tail, which can be expected, since the insulating phases cut off the correlations in the trapped system.

When the correlation function is Fourier transformed to get the momentum distribution, the difference at large distances in the correlation function gives a difference in the momentum distributions for small k values. The momentum distribution for the confined systems is compared with the momentum distribution for the homogeneous system in Fig. 10, and except for the peak value we notice a reasonable overall agreement.

Previous calculations have indicated that the appear-

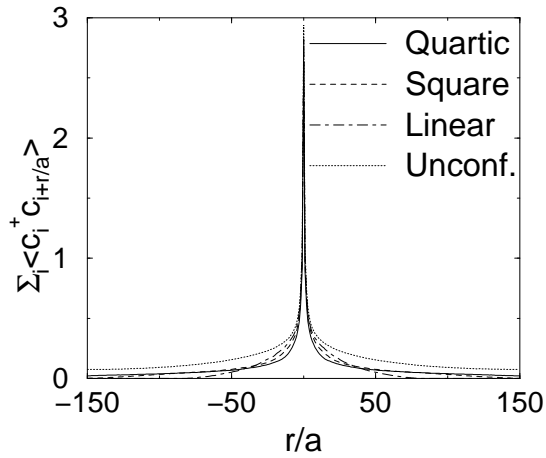


FIG. 9: The spatial average of the particle-particle correlation function for the confined system is compared with the value for the homogeneous system for $t/V = 0.1$.

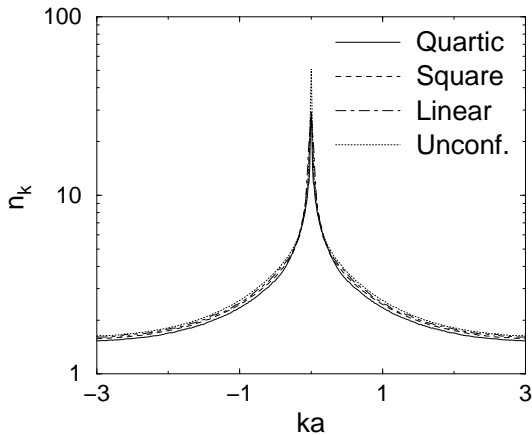


FIG. 10: The momentum distribution for the confined system is compared with the value for the homogeneous system for $t/V = 0.1$.

ance of a fine structure in the momentum distribution can be used to detect the formation of a Mott insulating plateau in the middle of the well.¹⁶ In another study the fine structure is claimed to be a finite-size effect.⁹ We observe fine structure in the Fourier transform of correlation functions originating from individual sites in the superfluid phase. This structure appears as a consequence of the abrupt cut in the correlation function obtained when the Mott insulating phases or the edges of the system are reached, as mentioned above. An example of this structure is shown in Fig. 11. However, the sum of all the correlations is smooth since the cutoff in the correlation functions appears at different distances for different lattice points. In case a small lattice is studied some fine structure may remain and this supports the earlier conclusion⁹ that the satellite peaks are a finite-size effect.

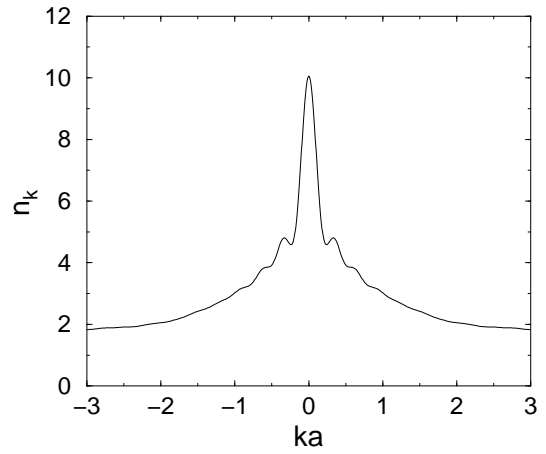


FIG. 11: An example of the fine structure when the particle-particle correlation function from one point in the superfluid phase is Fourier transformed.

IV. CONCLUSIONS

We examine the accuracy of a local-density approximation for the one-dimensional Bose-Hubbard model using a quantum Monte Carlo method. In this approximation the behavior of the confined system is approximated with that of the unconfined system. In most of the interesting parameter regime one can obtain quantitatively accurate results using this approximation. In this manner the state diagram for a confined system can be determined to a high degree of accuracy from knowledge of the phase diagram of the homogeneous Bose-Hubbard model. We demonstrate how the approximation fails where the correlation length diverges in the homogeneous system, and also when the local density varies rapidly from site to site. Even for the case of the nonlocal momentum distribution the local-density approximation works fairly well. Contrary to earlier studies we find no evidence of universal scaling as an insulating plateau is approached. Since the confined systems do not display a continuous phase transition this is to be expected. Finally, we provide more evidence for the case that an observed fine structure in the momentum distribution is related to a finite-size effect.

Acknowledgments

We are indebted to S. Wessel for instructive discussions on the local compressibility and to A. Sandvik and O. Syljuåsen for fruitful discussions. This work was supported by the Swedish Research Council and the Göran Gustafsson foundation.

* Electronic address: sara@theophys.kth.se

- ¹ D. Jaksch, C. Bruder, J. Cirac, C. Gardiner, and P. Zoller, Phys. Rev. Lett **81**, 3108 (1998).
- ² M. P. A. Fisher, P. B. Weichman, G. Grinstein, and D. S. Fisher, Phys. Rev. B **40**, 546 (1989).
- ³ G. G. Batrouni, R. T. Scalettar, and G. T. Zimanyi, Phys. Rev. Lett. **65**, 1765 (1990).
- ⁴ M. Greiner, O. Mandel, T. Esslinger, T. Hänsch, and I. Bloch, Nature **69**, 031601 (2002).
- ⁵ G. G. Batrouni, V. Rousseau, R. T. Scalettar, M. Rigol, A. Muramatsu, P. J. H. Denteneer, and M. Troyer, Phys. Rev. Lett **89**, 117203 (2002).
- ⁶ M. Rigol, A. Muramatsu, G. G. Batrouni, and R. T. Scalettar, Phys. Rev. Lett. **91**, 130403 (2003).
- ⁷ M. Rigol and A. Muramatsu, Phys. Rev. A **69**, 053612 (2004).
- ⁸ C. Kollath, U. Schollwöck, J. von Delft, and W. Zwerger, Phys. Rev. A **69**, 031601 (2004).
- ⁹ L. Pollet, S. Rombouts, K. Heyde, and J. Dukelsky, Phys. Rev. A **69**, 043601 (2004).
- ¹⁰ S. Wessel, F. Alet, M. Troyer, and G. G. Batrouni, Adv. Solid State Phys. **44**, 265 (2004).
- ¹¹ S. Wessel, F. Alet, M. Troyer, and G. G. Batrouni, cond-mat/0404552 (to appear in Phys. Rev. A).
- ¹² A. W. Sandvik, Phys. Rev. B **59**, R14157 (1999).
- ¹³ O. F. Syljuåsen and A. W. Sandvik, Phys. Rev. E **66**, 046701 (2002).
- ¹⁴ G. G. Batrouni and R. T. Scalettar, Phys. Rev. B **46**, 9051 (1992).
- ¹⁵ T. Kühner, S. R. White, and H. Monien, Phys. Rev. B **61**, 12474 (2000).
- ¹⁶ V. Kashurnikov, N. Prokof'ev, and B. Svistunov, Phys. Rev. A **66**, 031601 (2002).